From spreading depolarization to epilepsy with neuroinflammation: the role of CGRP in cortex

Fátima Gimeno-Ferrer, Annett Eitner, Reinhard Bauer, Alfred Lehmenkühler, Marie-Luise Edenhofer, Michaela Kress, Hans-Georg Schaible, Frank Richter

Angaben zur Veröffentlichung / Publication details:

Gimeno-Ferrer, Fátima, Annett Eitner, Reinhard Bauer, Alfred Lehmenkühler, Marie-Luise Edenhofer, Michaela Kress, Hans-Georg Schaible, and Frank Richter. 2022. "From spreading depolarization to epilepsy with neuroinflammation: the role of CGRP in cortex." Experimental Neurology 356: 114152. https://doi.org/10.1016/j.expneurol.2022.114152.

Experimental Neurology 356 (2022) 114152

Contents lists available at ScienceDirect

Experimental Neurology

journal homepage: www.elsevier.com/locate/yexnr

Research paper

From spreading depolarization to epilepsy with neuroinflammation: The role of CGRP in cortex

Fátima Gimeno-Ferrer [a], Annett Eitner [b], Reinhard Bauer [c], Alfred Lehmenkühler [d], Marie-Luise Edenhofer [e], Michaela Kress [e], Hans-Georg Schaible [a], Frank Richter [a,*]

[a] Institute of Physiology 1/Neurophysiology, Jena University Hospital, D-07740 Jena, Germany
[b] Department of Trauma, Hand and Reconstructive Surgery, Experimental Trauma Surgery, Jena University Hospital, D-07740 Jena, Germany
[c] Institute of Molecular Cell Biology, CMB-Center for Molecular Biomedicine, Jena University Hospital, D-07740 Jena, Germany
[d] Pain Institute & Center for Medical Education, D-40477 Düsseldorf, Germany
[e] Institute of Physiology, Medical University, Schöpfstraße 41, A-6020 Innsbruck, Austria

ARTICLE INFO

Keywords:
Calcitonin gene-related peptide
Epilepsy
Cortical spreading depolarization
Microglia
Blood-brain-barrier
Migraine

ABSTRACT

CGRP release plays a major role in migraine pain by activating the trigeminal pain pathways. Here we explored putative additional effects of CGRP on cortical circuits and investigated whether CGRP affects cortical excitability, cortical spreading depolarization (CSD), a phenomenon associated with migraine aura, blood-brain-barrier (BBB) and microglial morphology. We used immunohistochemistry to localize CGRP and the CGRP receptor (CGRP-R) in native cortex and evaluated morphology of microglia and integrity of the BBB after exposure to CGRP. In anesthetized rats we applied CGRP and the CGRP-R antagonist BIBN4096BS locally to the exposed cortex and monitored the spontaneous electrocorticogram and CSDs evoked by remote KCl pressure microinjection. In mouse brain slices CGRP effects on neuronal activity were explored by multielectrode array. CGRP immunoreactivity was detectable in intracortical vessels, and all cortical neurons showed CGRP-R immunoreactivity. In rat cortex in vivo, topical CGRP induced periods of epileptiform discharges, however, also dose-dependently reduced CSD amplitudes and propagation velocity. BIBN4096BS prevented these effects. CGRP evoked synchronized bursting activity in mouse cortical but not in cerebellar slices. Topical application of CGRP to rat cortex induced plasma extravasation and this was associated with reduced ramification of microglial cells. From these findings we conclude that CGRP induces a pathophysiological state in the cortex, consisting in neuronal hyperexcitability and neuroinflammation. Thus, CGRP may have a pronounced impact on brain functions during migraine episodes supporting the benefit of CGRP antagonists for clinical use. However, increased cortical CGRP may end the CSD-induced aura phase of migraine.

1. Introduction

Calcitonin gene-related peptide (CGRP) has a central role in migraine. The release of CGRP from peripheral and central branches of trigeminal neurons is thought to be of critical importance in the generation of migraine pain (Ferrari et al., 2022; Silberstein, 2004). Although sites and mechanisms of CGRP actions are a field of experimental and clinical research, novel therapies with antagonists and monoclonal antibodies targeting CGRP and CGRP receptors (CGRP-R) exhibit remarkable therapeutic success in the treatment of migraine (Taylor, 2019).

CGRP is a major neuropeptide in primary afferent trigeminal neurons, therefore, the focus of research on CGRP actions has been on the trigeminal pain pathway (Iyengar et al., 2019; Messlinger, 2018). However, CGRP may also have actions in the cortex because it is released from the meninges during migraine attacks (Iyengar et al., 2019). Furthermore, a localization of CGRP and CGRP-R was reported in cortical neurons (Warfvinge and Edvinsson, 2019). Therefore, putative

Abbreviations: CGRP, calcitonin gene-related peptide; CGRP-R, calcitonin gene-related peptide receptor; CSD, cortical spreading depolarization; BBB, blood-brain-barrier; CLR, calcitonin-like receptor; RAMP1, receptor activity-modifying protein 1; RCP, CGRP-receptor component protein; MEA, multielectrode array; DC, direct current; AC, alternate current; ECoG, electrocorticogram; EEG, electroencephalogram; rCBF, regional cerebral blood flow; LDF, laser Doppler flowmetry; IR, immunoreactivity; EB, Evans blue.

* Corresponding author at: Institute of Physiology 1/Neurophysiology, Jena University Hospital, Teichgraben 8, 07743 Jena, Germany.
E-mail address: Frank.Richter@med.uni-jena.de (F. Richter).

https://doi.org/10.1016/j.expneurol.2022.114152
Received 26 April 2022; Received in revised form 3 June 2022; Accepted 18 June 2022
Available online 26 June 2022

actions of CGRP in the cortex should be explored.

Related to migraine is the cortical spreading depolarization (CSD). This is an en masse depolarization of neurons and glial cells (Leao, 1944). Single CSDs are thought to be the basis of the migraine aura (Goadsby and Holland, 2019). Beyond migraine aura, repeated CSDs are thought to aggravate the consequences of ischemia and cerebrovascular stroke, because they are characterized by massive disturbances of ion and water homeostasis and energy consumption (Hartings et al., 2017). It was reported that CSD is also associated with CGRP since the release of this neuropeptide is induced after the occurrence of CSDs (Wang et al., 2019).

In the present study we addressed putative effects of CGRP on rodent cerebral cortex. Because molecular actions of CGRP are mediated by a CGRP-R, a heterodimer composed of CLR (calcitonin-like receptor) and RAMP1 (receptor activity-modifying protein 1) and the help of accessory protein RCP (CGRP-receptor component protein) (Russell et al., 2014), we investigated the expression of CLR in the cortex. We also studied the localization of CGRP in cortical tissue. Functionally, we explored in vivo whether local application of CGRP to the cortex influenced the occurrence and propagation of CSDs. The continuous recording from cortical areas allowed us to monitor abnormal discharge patterns such as episodes of epileptiform activity. Multielectrode array (MEA) recordings from mouse acute cortical and cerebellum slices were performed to study effects of CGRP on neuronal activity. Since CGRP causes inflammatory changes (neurogenic inflammation) (Russell et al., 2014), we further studied whether CGRP disturbed the blood-brain-barrier (BBB), and whether CGRP had an effect on microglia, a major contributor to neuroinflammation (Borst et al., 2021).

2. Methods

Experiments were approved by the Thuringian Government (Thüringer Landesamt für Verbraucherschutz). They were performed according to the Protection of Animals Act of the Federal Republic of Germany, in accordance with the declaration of Helsinki and the guiding principles in the care and use of animals. Data sampling, evaluation, and presentation complied with the ARRIVE guidelines.

2.1. Indirect immune fluorescence labeling for CGRP and CGRP-R location

Three control rats were perfused, using first PBS buffer under deep anesthesia, until euthanasia followed by perfusion with 4% ice-cold phosphate-buffered paraformaldehyde (PFA; Sigma-Aldrich). Brains were removed, post-fixed at least 24 h in 4% PFA, equilibrated in 30% sucrose, and frozen at −80 °C. Ten-μm-thick coronal sections were cut using a CM3050S cryostat (Leica Biosystems, Nussloch, Germany). Similarly, three native mouse brains were perfused, fixed, and sliced. Sections were incubated with primary antibodies over night at 4 °C and with secondary antibodies for 2 h at room temperature (Eitner et al., 2013). Sections were stained for identification of nuclei with Hoechst 34580 (1:500; Invitrogen, Darmstadt, Germany) and mounted on slides coverslipped with ProLong™ Gold Antifade Mountant (lnvitrogen, San Diego, CA). Primary antibodies were: mouse monoclonal anti-CGRP (1:100; Origene TA309091), rabbit anti-CALCR (CGRP-R) (1:50; Bioss bs-1860-r), mouse monoclonal anti-microtubule-associated protein 2 (MAP-2; 2a + 2b, 1:500; Sigma-Aldrich M1406), mouse anti-NeuN (1:100, Millipore MAB377), rabbit anti-Claudin-5 (CLDN5) (1:100, GeneTex GTX49371), rabbit anti-alpha-smooth-muscle-actin (α-SMA) (1:1000; Abcam ab5694), and goat anti-ionized calcium-binding adapter molecule 1 (Iba1, 1:200, GeneTex GTX89792). Secondary antibodies were conjugated with Alexa Fluor 488 or 568 (1:200; Invitrogen, San Diego). Control experiments were performed with omission of the primary antibodies. Sections were visualized using confocal laser scanning microscopy (TCS SP5, Leica). Contrast and brightness of the photomicrographs were adjusted using Adobe Photoshop CS5 (Adobe, San Jose, CA).

2.2. Surgical preparation of the rats

Adult male Wistar rats ($n = 45$; 350–450 g, aged 95 ± 4 days, housed in the Animal Facility of University Hospital Jena) were deeply anesthetized using sodium thiopental (Trapanal®; Inresa, Freiburg, Germany; 100–125 mg/kg intraperitoneally). During surgery, depth of anesthesia was regularly monitored by checking the absence of reflexes. Supplemental Trapanal (doses 20 mg/kg) maintained the depth of anesthesia. The trachea was cannulated to assist oxygenation; the right femoral artery to measure the mean arterial blood pressure. The electrocardiogram was continuously monitored. Body temperature was kept at 37 °C.

The head was fixed in a stereotactic holder. Using a minidrill, two trephinations over the left skull hemisphere exposed the brain (one rostral, spanning from 2 mm in rostral of Bregma over a length of 5–6 mm, 3–4 mm wide, and one more dorsal, 3–4 mm wide rostral of Lambda) while cooling with artificial cerebrospinal fluid (ACSF) (Richter et al., 2014; Richter et al., 2017). The ACSF contained (in mmol/L): NaCl 138.4, KCl 3.0, $CaCl_2$ 1.3, $MgCl_2$ 0.5, NaH_2PO_4 0.5, urea 2.2, and glucose 3.4, warmed to 37 °C and equilibrated with 5% CO_2 in O_2. The dura and arachnoidea underlying the trephinations were removed, the exposed cortex was kept moist with ACSF. Dental acrylic on the skull around the large frontal trephination formed a pool with a capacity for 100 μL for restricted topical application of test compounds.

2.3. Recording of intracortical direct current potentials, regional cerebral blood flow, and data processing in rat

We used an Ag/AgCl reference electrode (containing 2 mol/L KCl, placed on nasal bone), electrodes for direct current (DC) and electrocorticogram (ECoG) recordings (tip diameters approximately 5 μm, resistance <10 MΩ, filled with 150 mmol/L NaCl), an electrode for CSD elicitation (1 mol/L KCl), a double-barrelled electrode (one electrode for recording extracellular potassium concentration ($[K^+]_e$, one with NaCl as a reference). The ion-sensitive electrode barrel was backfilled with 100 mmol/L KCl, its tip was silanized (Selectophore, Sigma-Aldrich) and filled with K^+ ion changer (WPI 190, Sarasota, FL) (Nicholson, 1993).

Using a microinjector (picoinjector PLI-100; Harvard Apparatus, Holliston, MA), CSDs were elicited in the untreated cortex area by injection of 0.5 μL of 1 mol/L KCl solution with a pressure of 100 kPa. Starting from an injection time of 0.1 s, the injection time was increased in steps of 0.2 s at intervals of 3–5 min until CSDs were elicited twice (threshold determination). The signals were recorded with a 4-channel high-impedance amplifier (Meyer, Munich, Germany) and stored on a personal computer (sampling rate 2.048 Hz). CSDs were accepted if they had a steep onset between 1 and 3 s, reached amplitudes >5 mV, and propagated from electrode 1 to 4.

CSDs were evaluated as follows: elicitation yes/no, occurrence in the treated area, numbers after one microinjection, time interval between KCl microinjection and CSD peak in treated area (i.e. propagation time from the elicitation site (electrode DC 1) to the deepest electrode (electrode DC 3) in the treated area), and maximal amplitudes (baseline set before steep onset).

In each animal, initially two CSDs were elicited at intervals of 20 min to confirm the ability of the brain to produce CSD (control CSDs in the Figures). Then, CGRP dissolved in PBS, was applied to the treatment pool at either 10^{-5}, 10^{-6}, 10^{-7} or 10^{-8} mol/L (TOCRIS, Sigma-Aldrich, Taufkirchen, Germany) (one concentration per experiment). Thereafter, CSDs were elicited every 30 min for maximally 4 h. In addition, the regional cortical blood flow (rCBF) at the cerebral surface was measured continuously with a flow meter (Laser Blood Flow Monitor DRT4, sensor tip diameter approximately 1 mm, Moor Instruments, Millwey, Axminster, Devon, UK) in the treated and untreated areas (close to the DC recording electrodes, avoiding major blood vessels).

In some experiments, the CGRP-R antagonist, BIBN4096BS (Sigma-Aldrich, Taufkirchen) at 10^{-8} mol/L was applied topically to the cortex, either 2 h before CGRP 10^{-7} mol/L was administered and CSDs were elicited, or co-administered with CGRP for 4 h, and CSDs were elicited every half hour.

To analyze depression of the ECoG activity associated with spreading depolarization, DC recordings were resampled offline with a sample rate of 205 Hz and first detrended by appropriate adaptive filtering, followed by band pass filtering (bandpass 0.01–45 Hz). To reveal alternate current (AC)-ECoG activity, the signals were high-pass filtered with a lower frequency limit of 0.5 Hz. This evaluation allows identifying epileptiform EEG activity and seizures (Dreier et al., 2017).

2.4. Multielectrode array (MEA) recordings from brain slice preparations

We used male C57BL/6N mice ($n = 10$, aged 10–12 weeks, obtained from Charles River Laboratories, Sulzfeld, Germany). Mice were housed at 24 °C with ad libitum access to tap water and pelleted chow (Tagger, Austria), and individually housed for minimum 4 days before the experiments, which were performed during the light phase of the 12-h light/dark cycle.

For preparing coronal brain slices, the animals were anesthetized with isoflurane (IsoFlo®, Zoetis, Kalamazoo, MI) and decapitated. The brains were rapidly removed and immersed in ice-cold oxygenated (95% O_2, 5% CO_2) ACSF containing (in mmol/L): NaCl 125, $NaHC0_3$ 25, D-glucose 25, KCl 2.5, NaH_2PO_4 1.25, $CaCl_2$ 2 and $MgCl_2$ 1 (Bischofberger et al., 2006). The brains were trimmed with a scalpel blade and the remaining parts were glued onto the stage of a vibrating microtome (VTl000S, Leica Microsystems, Germany) to cut 300-μm-thick coronal slices from cortex in Bregma 0.00 mm and sagittal slices from cerebellar cortex. The cerebral cortex slices were incubated for 10–15 min in 32–34 °C oxygenated protective ACSF containing (in mmol/L): *N*-methyl-D-glucamine 110, HCl 110, KCl 2.5, NaH_2PO_4 1.2, $NaHCO_3$ 25, D-glucose 25, $MgSO_4$ 10 and $CaCl_2$ 0.5 (Ting et al., 2014). After recovery, they were transferred to ACSF at room temperature for at least 1 h before recordings. Cerebellar slices were transferred directly to normal ACSF for 1 h at room temperature after slicing.

For recordings, the slices were transferred to the 3D MEA chamber (120MEA-100/30iR-ITO, Quane Biosciences, Lausanne, Switzerland) and fixed with a platinum-framed grid with nylon fibers (weight ~ 0.3 g). The MEA was then inserted into the recording apparatus (MEA2100-System, Multi Channel Systems, Reutlingen, Germany). Using the Peristaltic Perfusion System 2 pump (PPS2, Multi Channel Systems), slices were superfused with oxygenated ACSF at 32–34 °C for 6 to 10 min baseline. Then CGRP (Phoenix Pharmaceuticals, Burlingame, CA) 10^{-7} or 10^{-6} mol/L in ACSF was perfused for 30–45 min, and finally CGRP was washed out with ACSF superfusion for 15–30 min.

Spontaneous action potential discharge activity was recorded with a sampling rate of 5 kHz. The position of the slices on the electrode field was photographed on an inverted microscope (Leica DMi 1, Wetzlar, Germany) using a digital camera after recording. The recorded traces were analyzed using MC_Rack software (Multi Channel Systems). Data streams were 200 Hz high-pass-filtered, and spike detection was performed with a threshold of 5 standard deviations from noise. Electrodes were assigned to the respective brain region on the photographs. Recording electrodes were classified as active if the spiking frequency exceeded 0.016 Hz. For evaluation, values in μV during the recordings were established using the Min-Max option in Spike analyzer for each electrode and mean value in μV/s was obtained to study the network effect. For heatmap representation of MEA data showing μV changes (colour intensity) in each electrode along the time-course of the experiments, Python programming language (Van Rossum and Drake Jr, 1995) was used with the Pandas (McKinney et al., 2010; Reback et al., 2020) and Seaborn (Waskom, 2021) libraries.

2.5. Microglia staining

Rats with CGRP 10^{-6} mol/L treatment for 4 h (left hemisphere treated, right hemisphere control; no electrodes) were perfused and the brains were fixed as described above. In 40-μm-thick cryostat slices microglia was stained using rabbit anti-Iba1 (1:200; Waco #019–19741; against synthetic peptide C-terminal of Iba1) as primary antibody. Stacking images of a set of images acquired every 1 μm of each section were taken from the confocal laser scanning microscope. For morphology evaluation (endpoints/cell and branch length/cell), quantification in pictures of 750 × 750 μm was performed following the protocol of Young and Morrison (2018) for Image J (Schneider et al., 2012). In this region of interest (ROI) numbers of cells in untreated and treated areas were counted for comparison.

2.6. Assessment of plasma extravasation

After completion of CSD recordings with CGRP (10^{-5} mol/L), animals received 0.5 mL of 4% Evans Blue (EB) (Sigma-Aldrich, Saint Louis) intravenously for 1 h. Fixed and frozen brains were cut in sequential 40-μm coronal sections and embedded in ProLong™ Gold Antifade Mountant. Images of plasma extravasation were monitored using confocal laser scanning microscopy. To evoke a fluorescence signal EB was excited with a diode-pumped solid-state laser at 561 nm. Fluorescence signals were recorded between 570 and 700 nm using a 20 × 0.7 dry objective. CD68 staining was performed with mouse anti-ED-1 monoclonal antibody (1:100; Bio-Rad MCA341R) to check macrophage infiltration. Rat spleen cryosections served as positive control. Evans Blue fluorescence intensity was quantified in a ROI of 70 × 70 μm (superior border located on the cortical surface), using ImageJ (Schneider et al., 2012).

2.7. Data statistics

Data are reported as mean ± standard error of the mean. For statistical analysis we used the InStat software package (Graph Pad, San Diego, CA), tested for normal distribution, and performed tests between groups (*t*-test, Student) as well as against a reference value (One-Sample t-test). Significance was accepted at $p < 0.05$.

3. Results

3.1. Expression of CGRP- and CGRP-R-immunoreactivity in rat cortex

In order to visualize putative sites of action of CGRP in the cortex, we studied the localization of CGRP- and CGRP-R-immunoreactivity (IR) by indirect immune fluorescence. We identified CGRP-IR co-localized with Claudin-5 (CLDN5) and alpha Smooth Muscle Actin (α-SMA) (Fig. 1A) suggesting that CGRP is present in cortical blood vessels (arteries and capillaries respectively), however not in cortical neurons. The CLR subunit of CGRP-R was found to be co-localized with neuronal nuclear protein (NeuN), being expressed by all cortical neurons (Fig. 1B). CLR showed also spots of co-localization with microtubule-associated protein 2 (MAP-2) which labels neuronal processes (Fig. 1B) (Dehmelt and Halpain, 2005). Therefore, CGRP-R was present in cortical neuronal somata and to some extent in neuronal processes.

3.2. CGRP effect on CSD

Application of CGRP to the treated area (Fig. 2A) directly induced CSDs only in 6 of 29 animals (21%, Table 1) suggesting that CGRP may elicit CSD, however, this effect was rare (for further details see below). In contrast, CGRP regularly modified the CSDs which were elicited by KCl microinjection into the untreated area and propagated into the treated area. Fig. 2B, left side, displays control CSD waves recorded at the electrodes 1 and 2 shortly after KCl microinjection, which were

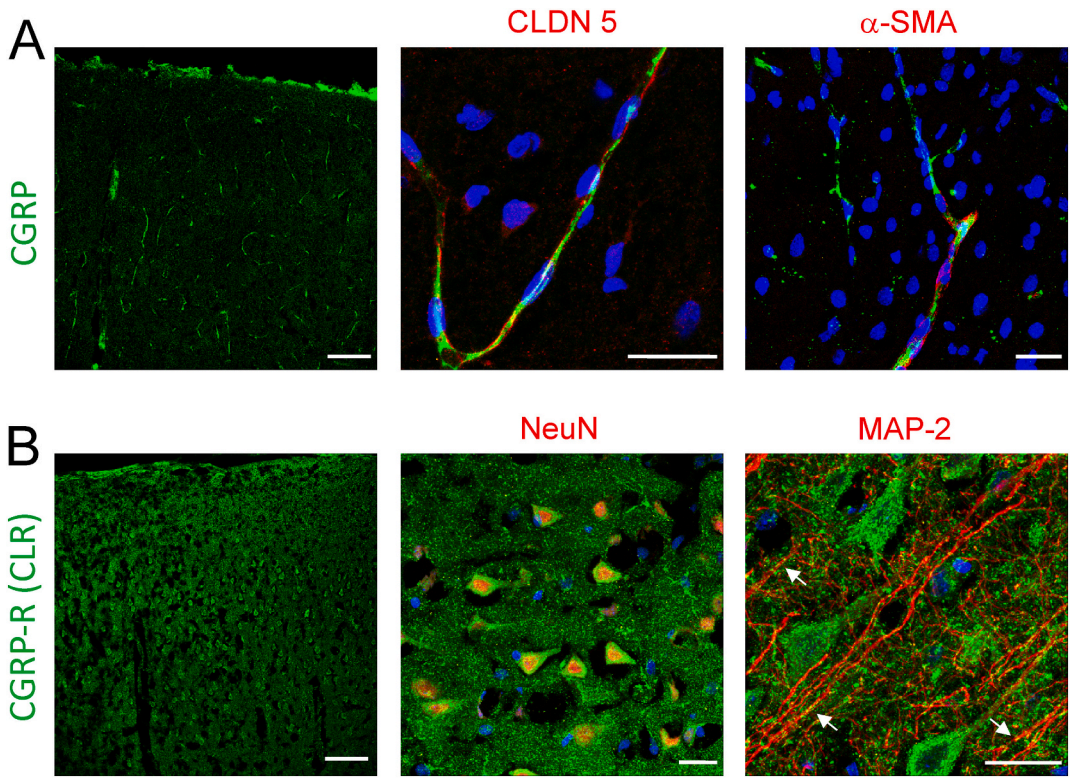

Fig. 1. Confocal fluorescent images of CGRP-IR and CLR-IR of CGRP-R in rat cortex. Left panels show an overview of rat cortex with surface facing upwards, middle and right panels show cortical areas with higher magnification. A) CGRP-IR (green) is located in cortical vessels, capillaries (colocalization with CLDN5, stained in red, middle panel) and in cortical arteries (colocalization with α-SMA, stained in red, right panel). B) CLR (stained in green) is located within somata of cortical neurons (colocalization with NeuN, stained in red, middle panel) and in spot-like colocalization with MAP-2, a marker for neuronal processes (stained in red, right panel). Nuclei are stained with Hoechst 34580 (blue). Scale bars for overview pictures 100 μm and for detailed pictures 25 μm. (For interpretation of the references to colour in this figure legend, the reader is referred to the web version of this article.)

accompanied and followed by depression of electroencephalographic activity (ECoG), transient increases of $[K^+]_e$ (linked to electrode 3), and increases of regional blood flow (rCBF). These CSDs arrived at the electrodes 3 (depth 1200 μm) and 4 (depth 400 μm) in the treated area after 2–5 min. Fig. 2B, right side, shows elicited CSDs four hours after CGRP application to the treated area. CSD amplitudes recorded at electrodes 3 and 4 were significantly reduced compared to the control period.

Data from all experiments are summarized in Fig. 3A-C. CGRP appeared to reduce CSD amplitudes in particular 4 h after CGRP application (Fig. 3A) in a dose-dependent manner ($p < 0.5$ for CGRP 10^{-5} and 10^{-6} mol/L, one sample *t*-test with reference value of 100% for control phase of the experiment). Brains treated with ACSF only showed some decline of amplitudes as well, but the reduction was smaller than after CGRP. Even in the untreated area a small but significant decrease of CSD amplitudes was observed after distant CGRP treatment at the two highest doses (CGRP 10^{-5} and 10^{-6} mol/L) (one sample t-test with reference value of 100% for control phase of the experiment, Fig. 3B). In addition, the propagation of CSDs from the untreated to the treated area exhibited a significant slowing after CGRP at 10^{-5}, 10^{-6}, and 10^{-8} mol/L (Fig. 3C).

3.3. CGRP effect on rat cortical excitability in vivo

Low-pass filter transformation of the DC into AC-ECoG revealed that topical application of CGRP to the treated area triggered episodes of local ictal discharge activity (Fig. 4A, electrode 4, ECoG). Table 1 displays the frequency of CSDs without KCl stimulus and of non-normal EEG after different doses of CGRP. Such epileptiform EEG activity could initially occur in addition to CSD (Fig. 4A, 30 min), but could also appear when CSDs were completely abolished in the treated area, while CSDs were still elicited in the untreated area (Fig. 4A, 240 min). This epileptiform activity appeared either as sharp-wave activity in the treated area, unrelated to CSD (Fig. 4B, 9 of 29 rats), or as bursting activity usually after a CSD (Fig. 4C, 9 of 29 rats).

3.4. The selective CGRP-R antagonist BIBN4096BS inhibits CGRP effects

The CGRP-R antagonist BIBN4096BS (Olcegepant®) has recently been launched for clinical use for the treatment of migraine (Hargreaves and Olesen, 2019). Local pretreatment with BIBN4096BS 10^{-8} mol/L for 2 h did not change CSD amplitude, nor did the subsequent CGRP 10^{-7} mol/L application for 2 h alter CSD amplitudes either ($n = 5$ rats, Fig. 4A). After coapplication of BIBN4096BS and CGRP the CSD amplitudes remained unaltered (n = 5, Fig. 5B). BIBN4096BS had an inconsistent effect on CSD propagation velocity. Neither an obvious change in the ECoG nor epileptiform activity was ever observed during these protocols suggesting that blockade of the CGRP-R prevented the generation of such discharge patterns.

3.5. CGRP effect on mouse brain excitability ex vivo

With immunohistochemistry, CGRP-R-IR was observed in mouse cortical neurons, and also in cerebellar neurons including Purkinje neurons (Fig. 6A, B). In MEA recordings from slices of the mouse cortex, CGRP was found to elicit episodes of synchronized activity (Fig. 6C). Such synchronized activity was observed after CGRP 10^{-6} and 10^{-7} mol/L (one concentration per slice, 5 slices from 5 different animals) throughout the CGRP application for 30 min. Washout of CGRP with ACSF for 30 min did not stop the synchronized activity. By contrast, even

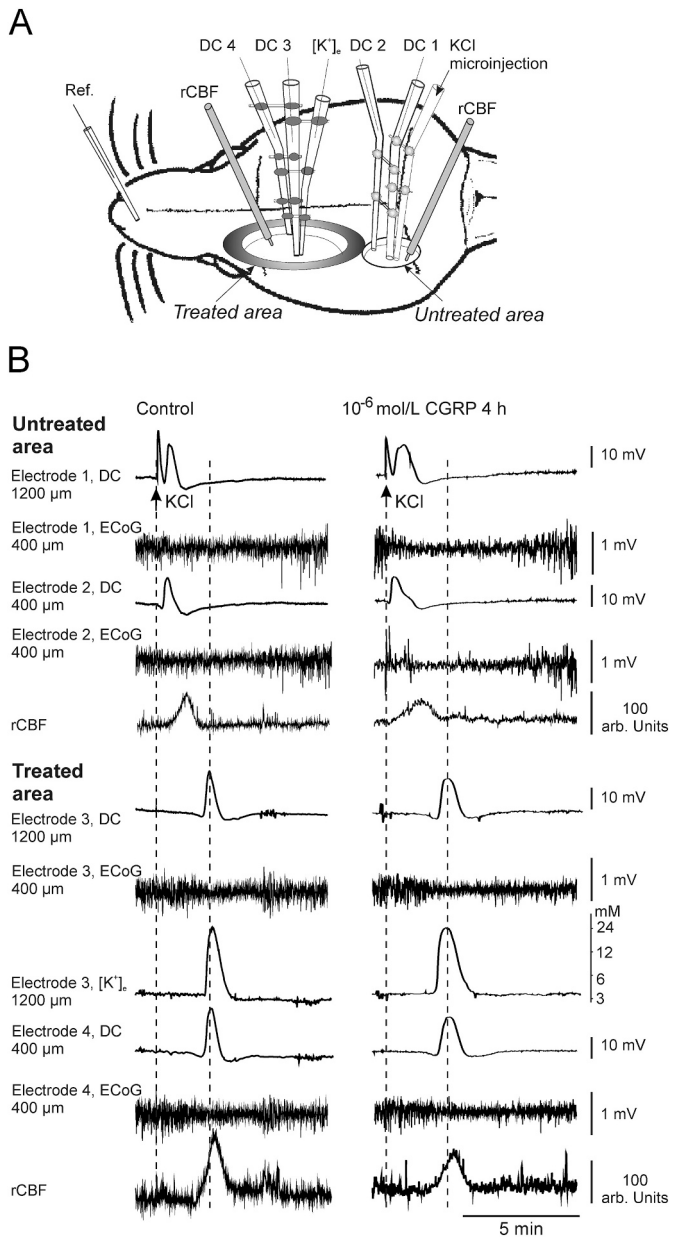

Fig. 2. Recordings from the rat cortex in vivo. A) Schematic drawing of the rat skull (not to scale) with the two trephinations and inserted electrodes and laser doppler probes for measuring regional cerebral blood flow (rCBF) in treated and untreated areas. B) Representative CSD recorded simultaneously with 5 electrodes (4 for DC-current and 1 for the associated increase in $[K^+]_e$) from treated and untreated brain areas before and 4 h after topical application of CGRP at 10^{-6} mol/L. Arrows mark the microinjection of KCl to elicit CSD. Dotted lines accentuate CSD propagation times from site of elicitation to treated area that was slowed after CGRP. The panels show the DC-electrocorticogram (DC-ECoG) and the respective high-pass filtered electrocorticographic data with a lower frequency limit of 0.5 Hz thus indicating that there is spreading depression of electroencephalographic activity.

CGRP application of 45 min to the cerebellum (10^{-6} and 10^{-7} mol/L, one concentration per slice, 3 slices from 3 animals) did not cause synchronized activity, most likely because most cerebellar CGRP-R-positive neurons are inhibitory (Fig. 6D).

3.6. Effects of CGRP on cortical blood-brain-barrier (BBB)

Evans Blue (EB) staining of slices from rat cortex showed that CGRP treatment for 4 h induced plasma extravasation presumably by breakdown of BBB (Fig. 7A). The EB fluorescence intensity was significantly higher in CGRP (10^{-5} mol/L)-treated areas than in untreated (ACSF) areas (Fig. 7B; $n = 3$ animals, 22 treated slices, 10 untreated slices, separated 100–200 µm). In order to check for cellular infiltration, we used the ED-1 antibody (labels the macrophage marker CD68) but did not find any labeling indicating that CGRP does not induce macrophage infiltration within 4 h.

Table 1
Occurrence of CSD without an ignition by KCl, and of non-normal electroencephalographic activity (ictal discharging activity or seizure activity) after topical application of CGRP in different concentrations alone. The numbers give the rats in which the effects were seen and the corresponding normalized percentage. No effects on EEG activity were detected neither after pretreatment nor in co-application of CGRP and BIBN4096BS.

Concentration of substances	No. of rats tested	No. of rats with observed events		
		CSD without KCl stimulus	Non-normal EEG activity	
			Ictal activity	Seizure activity
CGRP 10^{-5} mol/L	7	1	1	3
CGRP 10^{-6} mol/L	7	0	3	2
CGRP 10^{-7} mol/L	8	3	4	2
CGRP 10^{-8} mol/L	7	2	1	2
Total	29	6	9	9
		20.7%	31.0%	31.0%
			62.0%	
BIBN4096BS, then CGRP 10^{-7} mol/L	5	0	0	0
BIBN4096BS, + CGRP 10^{-7} mol/L	5	0	0	0

3.7. Morphological changes in microglia induced by CGRP

From the brains of 3 animals, we made 3 sections (separated 50–100 µm) from both the treated (CGRP 10^{-6} mol/L) and the control side (no electrodes inserted, no CSDs elicited). Microglia cells did not present CGRP-R-IR (Fig. 7C). Nevertheless, topical application of CGRP 10^{-6} mol/L for 4 h changed the morphology of microglial cells (Fig. 7D). It induced a statistically significant decrease in number of endpoints/cell of microglial processes (Fig. 7E) and in process length in microglia from the treated side compared to the untreated control side (Fig. 7F). However, no significant change in number of cells between treated and control side in a ROI of 750 × 750 µm was observed (Fig. 7G). Since microglial cells did not express CGRP-R, the morphological changes may be an indirect neuronal effect of CGRP.

4. Discussion

This study addressed important biological effects of CGRP in the cerebral cortex. CGRP induced short periods of epileptiform discharges indicating enhancement of excitability. Another major effect was the reduction of the amplitudes of CSDs evoked by remote potassium application. These effects were prevented by the CGRP-R antagonist BIBN4096BS. Furthermore, CGRP caused reduction of microglia ramification suggesting microglia activation, and plasma extravasation. Thus, CGRP caused pathological cortical hyperexcitability associated with signs of neuroinflammation. These CGRP effects may be important in migraine and other brain dysfunctions.

In the brain the neuropeptide CGRP was colocalized with α-SMA and CLDN5, suggesting that CGRP is present in cortical vessels (arteries and capillaries respectively), and this is in line with previous studies reporting CGRP localization in extracerebral vessels (Russell et al., 2014; Wimalawansa, 1996). Our results confirm the extensive presence

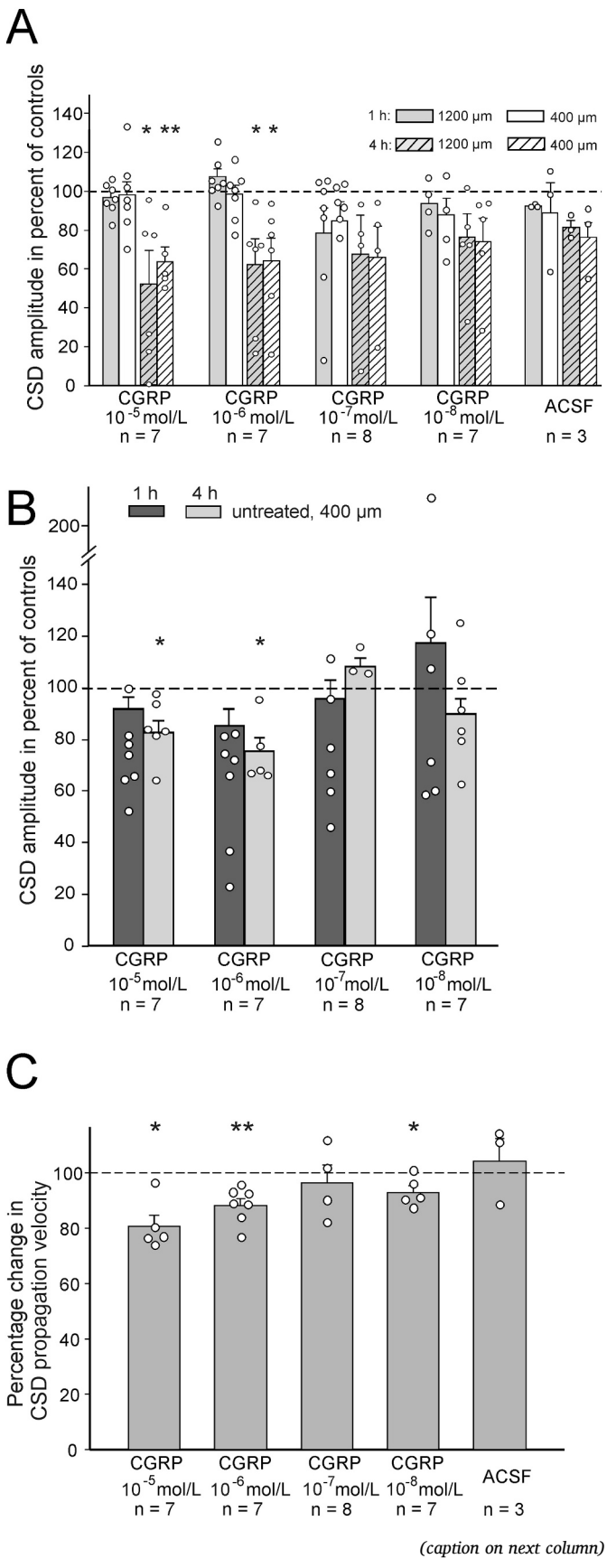

Fig. 3. Effect of CGRP on CSDs. A) Comparison of changes in CSD amplitudes at different depths (400 and 1200 µm from cortical surface) of the treated area 1 and 4 h after topical application of different concentrations of CGRP. Comparison with a group treated only with ACSF at both treated and untreated areas. Bars show mean values ± standard error, dots show single data points, n gives numbers of rats as in B and C. Statistical comparisons versus control CSDs (set at 100%, dashed line) were made with the one sample *t*-test, 1 symbol ($p < 0.05$), 2 symbols ($p < 0.01$). Differences of the numbers of data points between 1 and 4 h are due to electrode failure or development of epilepsy in treated area. B) Comparison of changes in CSD amplitudes 1 and 4 h in untreated area after topical application of CGRP at different concentrations to the remote treated area. Same type of display as in A. C) Application of CGRP at different concentrations resulted in a slowing of CSD propagation. The columns show mean values ± standard errors, dots show single data points, statistical comparisons of velocity at 4 h versus control CSDs were made with the paired t-test, 1 symbol ($p < 0.05$), 2 symbols ($p < 0.01$). Differences in the number of data points number of rats and 4 h are due to electrode failure (in treated and/or untreated) or development of epilepsy (in treated).

of CLR-IR in the cortex (Warfvinge and Edvinsson, 2019). Apparently, all cortical neurons expressed CGRP-R, and labelling for CLR was strong in the cortical somata but spots of coexpression of CLR and MAP-2 indicate some CLR expression also in neuronal processes. Thus, cortical neurons may be targeted by CGRP released from the meninges and from intracerebral vessels by volume transmission (Syková, 2004).

Previous studies reported that the experimental induction of CSD was followed by enhanced release of CGRP (Wang et al., 2019), but the consecutive effects of CGRP release are unknown to date. Therefore, we explored whether topical application of CGRP to the cortex in turn affected CSD. We applied CGRP at physiological amounts of CGRP (10^{-8} mol/L) and at higher doses (10^{-5} to 10^{-7} mol/L) as they occur during migraine attacks (Risch et al., 2021). Consistently, only in few cases, CGRP evoked CSD by itself but higher doses reduced the amplitudes of CSDs evoked remotely by K^+ application. Small CSD amplitude reductions in the untreated area were probably caused by leaking from the treated area underneath the skull bone or by expansive effects of CGRP. The amplitude reduction was prevented by the selective CGRP-R antagonist BIBN4096BS suggesting a self-limiting feedback loop, dependent on neuronal CGRP receptors. Because the aura phase is typically terminated in the pain phase, the release of CGRP by activation of the trigeminal system could be a mechanism that suppresses CSD generation. The induction of plasma extravasation by CGRP may contribute to the reduction of CSD amplitude and velocity because the changes of the extracellular milieu may influence the homeostatic conditions required for CSD propagation.

However, the net effect of CGRP itself in the cortex was excitatory, as evident from the recordings from slices of mouse cortex in which application of CGRP evoked periods of synchronized activity. Such excitatory effects of CGRP, producing repetitive action potentials were also observed in immature rat spinal dorsal horn neurons (Ryu et al., 1988), in neurons of rat amygdala (Han et al., 2010), and in mouse neurons of medullary slices (Zheng et al., 2021). Bursting activity in neuronal circuits may be mediated by enhanced activation of excitatory neurons via modulation of glutamate (both AMPA and NMDA) receptors, because CGRP enhances the responses of neurons to AMPA and NMDA application (Ebersberger et al., 2000; Teppola et al., 2019). Since apparently all neurons expressed CLR, CGRP most likely also activated inhibitory interneurons. If they are excited by CGRP, they may be more responsive to excitatory inputs and release more GABA thus possibly terminating synchronized activity. However, currently the precise CGRP mechanisms remain unclear. CGRP receptors are not only coupled to G_s proteins (which is considered the main pathway), they can also be coupled to G_i proteins and $G_{q/11}$ proteins (Cottrell, 2019). Currently it is unknown whether all of these cellular pathways are important in the cortex, and if so, in which types of neurons they may be expressed and which functions they support.

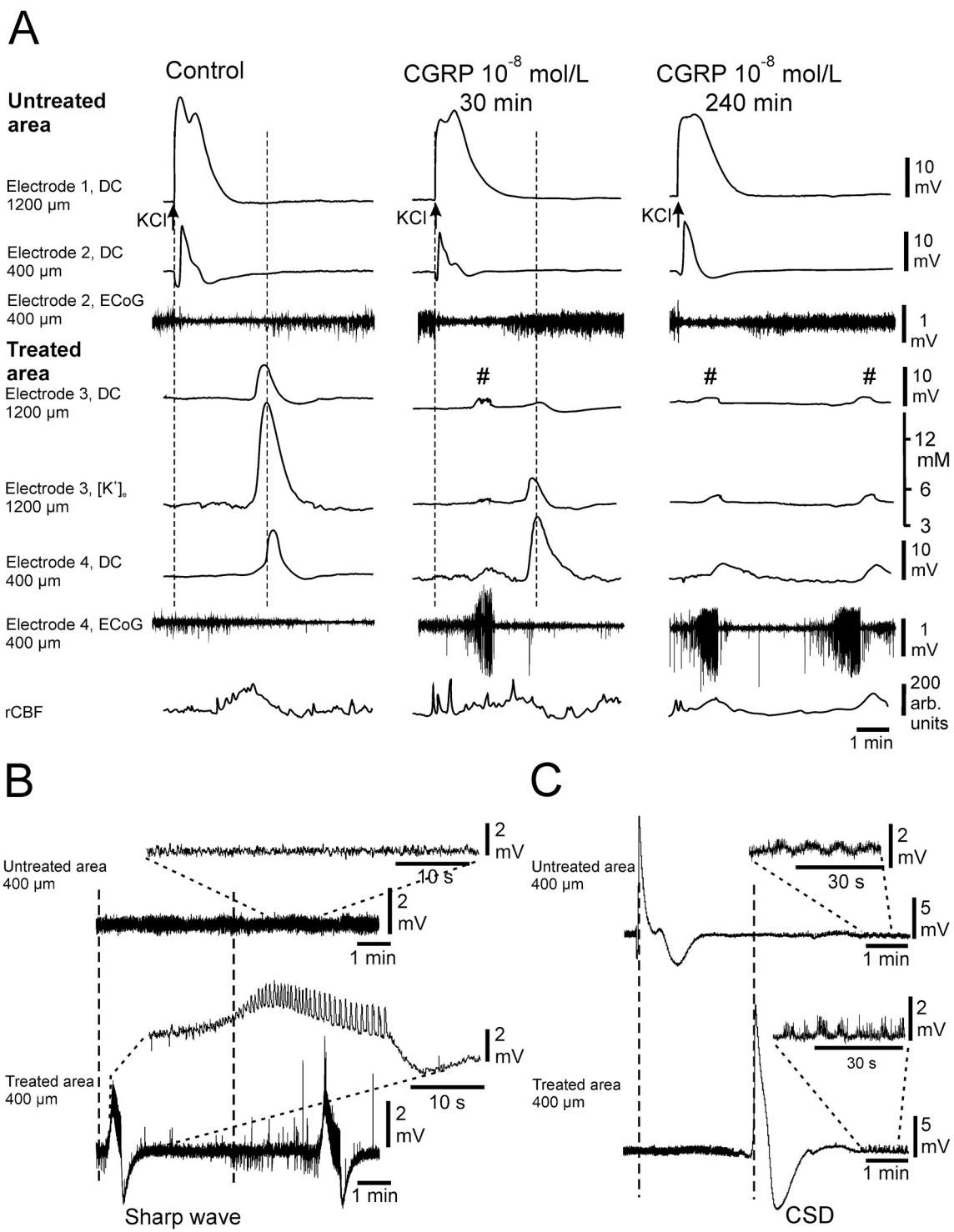

Fig. 4. Development of epileptic activity after CGRP. A) CSD samples with development of spontaneous ictal discharging activity (marked by #) when CGRP was applied at 10^{-8} mol/L. Arrows mark the microinjection of KCl to elicit CSD. Dotted lines accentuate CSD propagation times from site of elicitation to treated area. In untreated area KCl always elicited a propagating CSD wave. Both ictal discharges and CSD 30 min after CGRP application in the treated area, only ictal discharges after 4 h of CGRP treatment. B) Example trace of low-pass-filtered ECoG showing development of repetitive seizure activity after a sharp wave restricted to the area treated with CGRP which is absent at the untreated area with the corresponding magnification. C) Example trace of low-pass-filtered ECoG showing development of epileptiform activity after CSD in the area treated with CGRP, no seizure activity in the untreated area with the corresponding magnification.

Neuronal hyperexcitability is thought to be the basis for both spreading depression and epileptic discharges and seizures (Aronica and Mühlebner, 2017; Patel et al., 2019; Vinogradova, 2018). Whereas in spreading depolarization the excitation wave depolarizes a large number of neurons at once thereby causing a propagation of the wave in a directed manner, in epileptic foci neurons discharge in a random order thereby disrupting the balance between excitation and inhibition (Patel et al., 2019). In the present experiments, the episodic epileptiform discharges after CGRP usually appeared in the course of the experiments in which CSDs were elicited once per 30 min and were even observed at

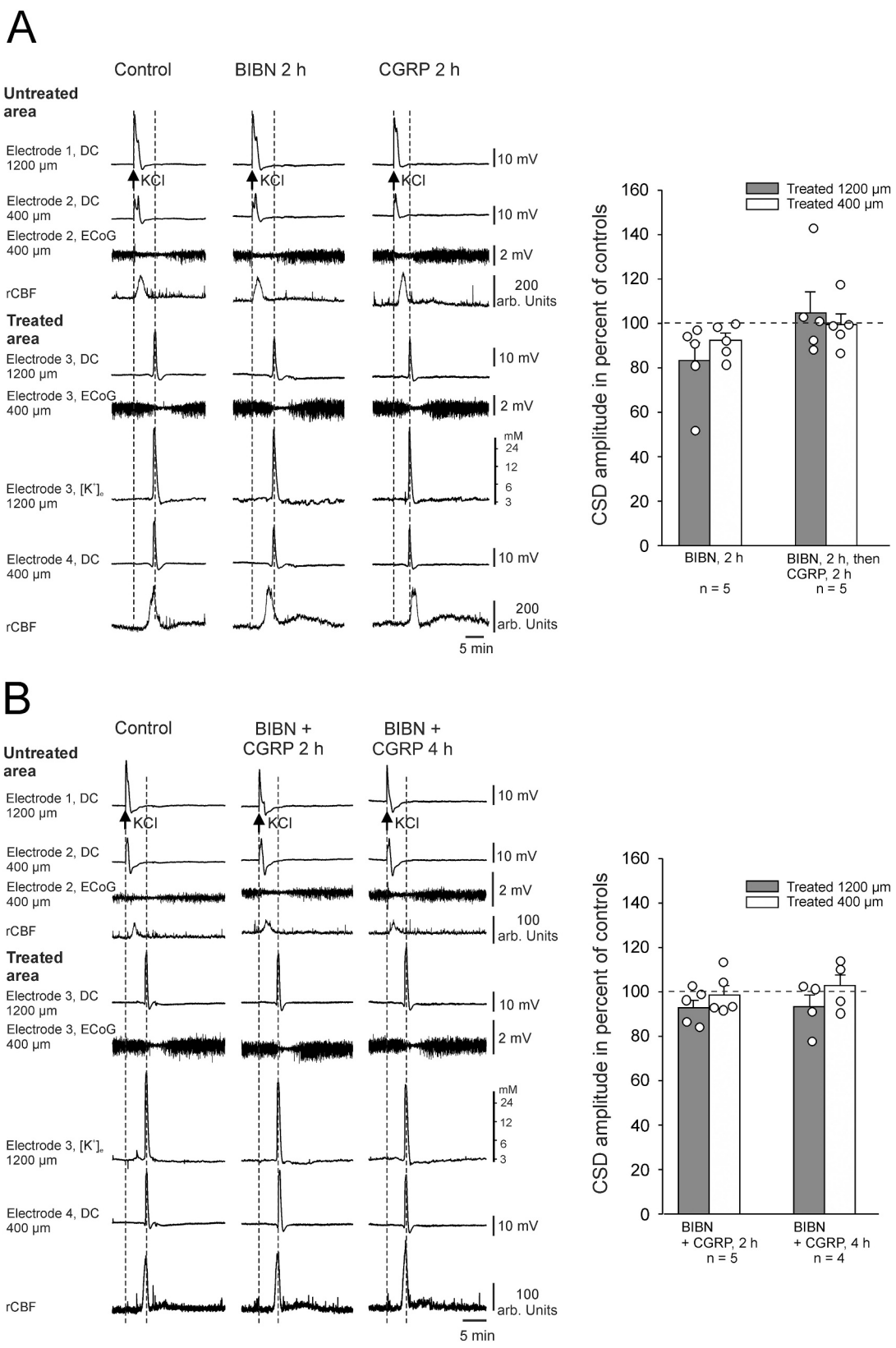

Fig. 5. Effect of BIBN4096BS on CSDs. A) Typical sample of CSD before and after pretreatment with BIBN4096BS for 2 h followed by 2 h of topical application of CGRP. Bar graph shows the comparison of effects of BIBN4096BS alone for 2 h, its preventive effect over CGRP (2 h BIBN4096BS + 2 h CGRP) expressed in percentage compared to controls (dashed line). The columns show mean values ± standard errors. Dots show single data points, n gives numbers of rats. No statistically significant differences. B) Typical sample of CSD before and after co-application of BIBN4096BS together with CGRP for 2 h and 4 h. Bar graph shows the comparison of effects of BIBN409BS after 2 h and 4 h in co-application with CGRP on CSD amplitudes. The columns show mean values ± standard errors, n gives numbers of rats. Dots show single data points. No statistically significant differences.

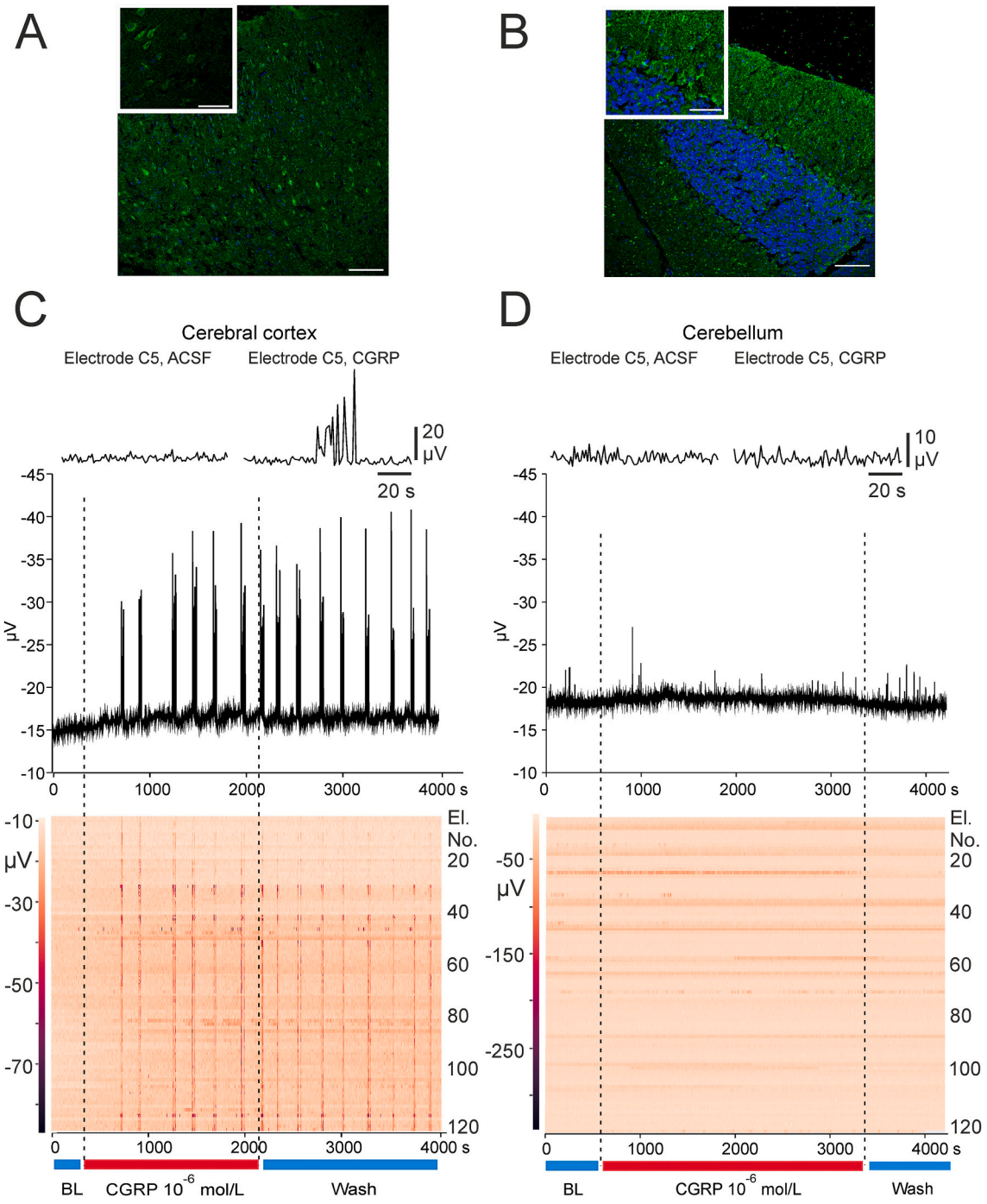

Fig. 6. MEA-recordings from cortical and cerebellar adult mouse brain slices. A) Localization of the CLR subunit of CGRP-R in all cortical neurons in mouse brain (in green). B) Localization of the CLR subunit of CGRP-R in Purkinje neurons and molecular layer in mouse cerebellum (in green). Scale bars are 50 µm for the detailed caption and 100 µm for the overview picture. C) CGRP induced repetitive discharging activity in mouse cortex recorded by MEA, the discharging effect was not removed with ACSF wash. The top curves show example traces of a single electrode before and after CGRP treatment, with the remarkable ictal-like activity induced by CGRP. The middle diagram shows the mean value in voltage from all electrodes over the time course of the recording (BL – baseline, then CGRP 10^{-6} mol/L for 30 min, followed by wash for 30 min). Heatmap at the bottom represents in horizontal direction the voltage changes according to time course of each electrode of the 120-electrode array displayed in vertical direction. Colour intensity shows µV change of each electrode. D) CGRP did not induce any remarkable change in excitation that could be recorded by MEA in cerebellum. Protocol has 45 min of CGRP application and 15 min wash. Cerebellum presents spontaneous activity of Purkinje neurons since the beginning, but firing was not affected or changed by CGRP application. (For interpretation of the references to colour in this figure legend, the reader is referred to the web version of this article.)

physiological doses of CGRP. Monitoring of neuronal activity for 4 h showed that initially epileptiform discharges and CSDs "coexisted" in the treated area. However, with increasing epileptiform activity, CSDs disappeared in the treated area, and CSDs, evoked outside of the treated area, did no longer propagate into the treated area. Several studies have addressed the relationship between CSDs and epileptiform discharges. On one hand, Koroleva and Bures (1980) reported that CSD does not migrate into epileptic foci in the brain. On the other hand, CSD can be induced by seizure-like activities (Broberg et al., 2008; Hablitz and Heinemann, 1989; Olsson et al., 2006). In the present experiments CSDs

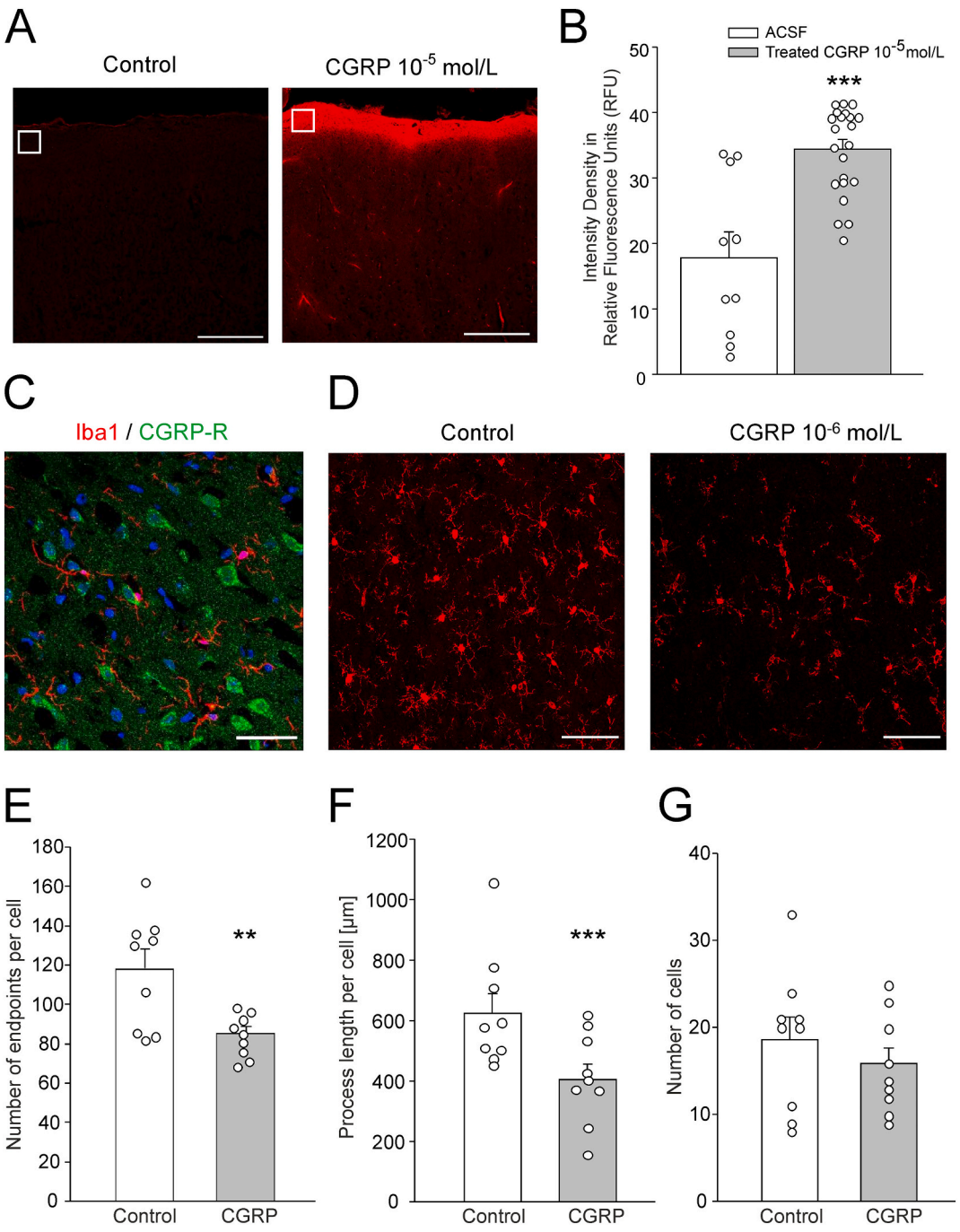

Fig. 7. Effects of CGRP on BBB and brain neuroinflammation parameters. A) Induction of plasma extravasation by topical application of CGRP 10^{-5} mol/L for 4 h, visualized by EB. Scale bars 200 µm. B) Quantification of plasma extravasation by measuring intensity of fluorescence in CGRP-treated (10^{-5} mol/L) and untreated brain areas in a ROI of 70 × 70 µm. C) No colocalization of CGRP-R-IR (in green) on cortical microglia stained with Iba1 (in red), scale bar 50 µm. D) Iba1-Immunofluorescence after application of CGRP at 10^{-6} mol/L for 4 h revealed a change in microglia morphology. Scale bars 100 µm. E) Quantification of endpoints/cell in microglia of areas treated with CGRP 10^{-6} mol/L and untreated areas in a ROI of 750 × 750 µm. F) Quantification of process length/cell in microglia of areas treated with CGRP 10^{-6} mol/L and untreated areas in the same ROI. G) Quantification of number of microglial cells in areas treated with CGRP 10^{-6} mol/L and untreated areas in the same ROI. In B), E), F) and G), bar graphs show the comparison between untreated and treated area with CGRP after 4 h. The columns show mean values ± standard errors. Dots show single data points. Statistical comparisons versus controls were made with the paired t-test, ** ($p < 0.01$), *** ($p < 0.001$). (For interpretation of the references to colour in this figure legend, the reader is referred to the web version of this article.)

were not triggered by epileptiform discharges. We were interested in checking for occurrence of synchronized activity in mouse cortical slice preparations. With the MEA technique we observed an increase in neuronal activity triggered by CGRP without any other stimulation (neither humoral, nor chemical or electrical).

The occurrence of epileptiform activity after CGRP application supports the concept of "migralepsy" which describes the coexistence of migraine and epilepsy (Demarquay and Rheims, 2021). A causal role of CGRP for the epileptiform episodes is very likely because epileptic discharges were not observed in rats in which the selective CGRP-R antagonist BIBN4096BS was administered before or during CGRP application.

Another novel finding was the effect of CGRP on microglia. Local treatment of CGRP induced on the treated side morphological changes of

microglial cells (decrease in number of process endpoints/cell and reduction of process length which characterize microglial affection) (Borst et al., 2021). Thus, CGRP application on the cortex may initiate transient neuroinflammation. It is unlikely that CGRP stimulated microglia directly because we did not identify CGRP-R on microglial cells. Importantly, we did not find macrophage invasion within the observation time, and thus this microglial effect evoked by acute CGRP application may not be as severe as in brain injuries. The particular mechanism, how CGRP may affect microglia, is still unclear. We speculate that mediators like the cytokine IL-1β that is known to be released from satellite cells in trigeminal ganglion (Thalakoti et al., 2007), or the messenger nitric oxide (NO) that is known to be produced by CGRP stimulation (Li et al., 2008) might have an impact on microglia as well as on vascular permeability. The activation of microglia may have many implications. An opening of the BBB is probably caused by the release of neuroinflammatory mediators from activated microglial cells (Edvinsson et al., 2019). Activated microglia may produce proinflammatory cytokines such as IL-1β that is known to diminish CSD amplitudes (Richter et al., 2017). It is likely that the binding of CGRP to neuronal receptors facilitates the production of cAMP (Cottrell, 2019) that could induce a higher rectifying potassium conductance (Shibata and Suzuki, 2017) together with a higher pumping activity of the Na^+/K^+ ATPase, thereby removing extracellular potassium more quickly, and this mechanism may also reduce CSD amplitudes. More work is necessary to understand the putative role of cortical microglial affection in the context of CGRP stimulation.

While the present study focused on the role of CGRP in migraine, other reports proposed a role of CGRP in other brain diseases. The CGRP-R antagonist BIBN4096BS ameliorated the development of Alzheimer's disease in young mice by decreasing neuroinflammatory markers (Na et al., 2020) supporting a role of CGRP in neuroinflammation. On the other hand, CGRP was shown to protect the brain in ischemic conditions (Lu et al., 2017; Rehni et al., 2008; Saklani et al., 2022) which may indicate that CGRP in blood vessels supports cerebral perfusion. Together, these data suggest an important role of CGRP both in the regulation of neuronal excitability and in the regulation of brain blood flow and brain homeostasis. In addition to CGRP, other neuropeptides such as substance P (Richter et al., 2018) or galanin (Shimazaki et al., 2022) may be involved in brain diseases and cooperate with CGRP.

5. Conclusions

The present study shows that apparently all cortical neurons express CGRP-R suggesting a role of CGRP in neuronal activity. Since local application of CGRP to the cortex induced cortical hyperexcitability to become manifest in episodic epileptiform discharges, and evoked neuroinflammation by breakdown of BBB and indirect microglial affection (reduced ramification) we propose that CGRP has an important role in the pathophysiology of migraine. In brain slices, CGRP evoked bursting activity showing excitatory functions. Enhanced excitability by CGRP may contribute to the general brain hyperexcitability during migraine episodes (Ferrari et al., 2015) which may become manifest in phonophobia, photophobia, dizziness (Silberstein, 1995), marching paraesthesias (Petrusic et al., 2013) or hyperosmia (Kelman, 2004). CGRP also reduced the amplitudes of CSDs or even prevented them, suggesting that increased cortical CGRP may limit the CSD-induced aura phase of migraine. These CGRP-induced effects were prevented by the CGRP-R antagonist BIBN4096BS supporting the benefit of CGRP antagonists for clinical use. Whether "normal" excitability is influenced by CGRP is unknown. In the present experiments the application of BIBN4096BS alone did not alter EEG patterns but EEG recordings may not be sensitive enough to reveal physiological CGRP functions. The localization of CGRP within intracerebral vessels and the presence of CGRP-R on the neurons suggest a functional connection between vessels and neurons (possible role of volume transmission). However, it remains to be investigated under which circumstances CGRP is released from intracerebral vessels.

CRediT authorship contribution statement

Fátima Gimeno-Ferrer: Conceptualization, Methodology, Investigation, Formal analysis, Writing – original draft. **Annett Eitner:** Conceptualization, Methodology, Investigation, Formal analysis, Writing – original draft. **Reinhard Bauer:** Methodology, Investigation, Formal analysis, Writing – original draft. **Alfred Lehmenkühler:** Conceptualization, Methodology, Writing – original draft. **Marie-Luise Edenhofer:** Methodology, Investigation, Formal analysis, Writing – original draft. **Michaela Kress:** Conceptualization, Methodology, Investigation, Formal analysis, Writing – original draft, Supervision, Funding acquisition. **Hans-Georg Schaible:** Conceptualization, Methodology, Investigation, Formal analysis, Writing – original draft, Supervision, Funding acquisition. **Frank Richter:** Conceptualization, Methodology, Investigation, Formal analysis, Writing – original draft, Supervision, Funding acquisition.

Declaration of Competing Interest

All authors have nothing to report.

Acknowledgements

We thank Mrs. Konstanze Ernst and Mrs. Rose-Marie Zimmer for excellent technical assistance. This project has received funding from the European Union's Horizon 2020 research and innovation programme under the Marie Skłodowska-Curie grant agreement No 764860.

References

Aronica, E., Mühlebner, A., 2017. Neuropathology of epilepsy. Handb. Clin. Neurol. 145, 193–216. https://doi.org/10.1016/B978-0-12-802395-2.00015-8.

Bischofberger, J., Engel, D., Li, L., Geiger, J.R., Jonas, P., 2006. Patch-clamp recording from mossy fiber terminals in hippocampal slices. Nat. Protoc. 1, 2075–2081. https://doi.org/10.1038/nprot.2006.312.

Borst, K., Dumas, A.A., Prinz, M., 2021. Microglia: Immune and non-immune functions. Immunity. 54, 2194–2208. https://doi.org/10.1016/j.immuni.2021.09.014.

Broberg, M., Pope, K.J., Lewis, T., Olsson, T., Nilsson, M., Willoughby, J.O., 2008. Cell swelling precedes seizures induced by inhibition of astrocytic metabolism. Epilepsy Res. 80, 132–141. https://doi.org/10.1016/j.eplepsyres.2008.03.012.

Cottrell, G.S., 2019. CGRP receptor signalling pathways. Handb. Exp. Pharmacol. 255, 37–64. https://doi.org/10.1007/164_2018_130.

Dehmelt, L., Halpain, S., 2005. The MAP2/Tau family of microtubule-associated proteins. Genome Biol. 6, 204. https://doi.org/10.1186/gb-2004-6-1-204.

Demarquay, G., Rheims, S., 2021. Relationships between migraine and epilepsy: pathophysiological mechanisms and clinical implications. Rev. Neurol. (Paris) 177, 791–800. https://doi.org/10.1016/j.neurol.2021.06.004.

Dreier, J.P., Fabricius, M., Ayata, C., Sakowitz, O.W., Shuttleworth, C.W., Dohmen, C., Graf, R., Vajkoczy, P., Helbok, R., Suzuki, M., Schiefecker, A.J., Major, S., Winkler, M.K., Kang, E.J., Milakara, D., Oliveira-Ferreira, A.I., Reiffurth, C., Revankar, G.S., Sugimoto, K., Dengler, N.F., Hecht, N., Foreman, B., Feyen, B., Kondziella, D., Friberg, C.K., Piilgaard, H., Rosenthal, E.S., Westover, M.B., Maslarova, A., Santos, E., Hertle, D., Sánchez-Porras, R., Jewell, S.L., Balança, B., Platz, J., Hinzman, J.M., Lückl, J., Schoknecht, K., Schöll, M., Drenckhahn, C., Feuerstein, D., Eriksen, N., Horst, V., Bretz, J.S., Jahnke, P., Scheel, M., Bohner, G., Rostrup, E., Pakkenberg, B., Heinemann, U., Claassen, J., Carlson, A.P., Kowoll, C. M., Lublinsky, S., Chassidim, Y., Shelef, I., Friedman, A., Brinker, G., Reiner, M., Kirov, S.A., Andrew, R.D., Farkas, E., Güresir, E., Vatter, H., Chung, L.S., Brennan, K. C., Lieutaud, T., Marinesco, S., Maas, A.I., Sahuquillo, J., Dahlem, M.A., Richter, F., Herreras, O., Boutelle, M.G., Okonkwo, D.O., Bullock, M.R., Witte, O.W., Martus, P., van den Maagdenberg, A.M., Ferrari, M.D., Dijkhuizen, R.M., Shutter, L.A., Andaluz, N., Schulte, A.P., MacVicar, B., Watanabe, T., Woitzik, J., Lauritzen, M., Strong, A.J., Hartings, J.A., 2017. Recording, analysis, and interpretation of spreading depolarizations in neurointensive care: review and recommendations of the COSBID research group. J. Cereb. Blood Flow Metab. 37, 1595–1625. https://doi.org/10.1177/0271678X16654496.

Ebersberger, A., Charbel Issa, P., Vanegas, H., Schaible, H.G., 2000. Differential effects of calcitonin gene-related peptide and calcitonin gene-related peptide 8-37 upon responses to N-methyl-D-aspartate or (R, S)-alpha-amino-3-hydroxy-5-methylisoxazole-4-propionate in spinal nociceptive neurons with knee joint input in the rat. Neuroscience. 99, 171–178. https://doi.org/10.1016/s0306-4522(00)00176-7.

Edvinsson, L., Haanes, K.A., Warfvinge, K., 2019. Does inflammation have a role in migraine? Nat. Rev. Neurol. 15, 483–490. https://doi.org/10.1038/s41582-019-0216-y.

Eitner, A., Pester, J., Nietzsche, S., Hofmann, G.O., Schaible, H.G., 2013. The innervation of synovium of human osteoarthritic joints in comparison with normal rat and sheep synovium. Osteoarthr. Cartil. 21, 1383–1391. https://doi.org/10.1016/j.joca.2013.06.018.

Ferrari, M.D., Klever, R.R., Terwindt, G.M., Ayata, C., van den Maagdenberg, A.M., 2015. Migraine pathophysiology: lessons from mouse models and human genetics. Lancet Neurol. 14, 65–80. https://doi.org/10.1016/S1474-4422(14)70220-0.

Ferrari, M.D., Goadsby, P.J., Burstein, R., Kurth, T., Ayata, C., Charles, A., Ashina, M., van den Maagdenberg, A.M.J.M., Dodick, D.W., 2022. Migraine. Nat. Rev. Dis. Prim. 8, 2. https://doi.org/10.1038/s41572-021-00328-4.

Goadsby, P.J., Holland, P.R., 2019. An update: pathophysiology of migraine. Neurol. Clin. 37, 651–671. https://doi.org/10.1016/j.ncl.2019.07.008.

Hablitz, J.J., Heinemann, U., 1989. Alterations in the microenvironment during spreading depression associated with epileptiform activity in the immature neocortex. Brain Res. Dev. Brain Res. 46, 243–252. https://doi.org/10.1016/0165-3806(89)90288-5.

Han, J.S., Adwanikar, H., Li, Z., Ji, G., Neugebauer, V., 2010. Facilitation of synaptic transmission and pain responses by CGRP in the amygdala of normal rats. Mol. Pain 6, 10. https://doi.org/10.1186/1744-8069-6-10.

Hargreaves, R., Olesen, J., 2019. Calcitonin gene-related peptide modulators - The history and renaissance of a new migraine drug class. Headache. 59, 951–970. https://doi.org/10.1111/head.13510.

Hartings, J.A., Shuttleworth, C.W., Kirov, S.A., Ayata, C., Hinzman, J.M., Foreman, B., Andrew, R.D., Boutelle, M.G., Brennan, K.C., Carlson, A.P., Dahlem, M.A., Drenckhahn, C., Dohmen, C., Fabricius, M., Farkas, E., Feuerstein, D., Graf, R., Helbok, R., Lauritzen, M., Major, S., Oliveira-Ferreira, A.I., Richter, F., Rosenthal, E. S., Sakowitz, O.W., Sánchez-Porras, R., Santos, E., Schöll, M., Strong, A.J., Urbach, A., Westover, M.B., Winkler, M.K., Witte, O.W., Woitzik, J., Dreier, J.P., 2017. The continuum of spreading depolarizations in acute cortical lesion development: examining Leão's legacy. J. Cereb. Blood Flow Metab. 37, 1571–1594. https://doi.org/10.1177/0271678X16654495.

Iyengar, S., Johnson, K.W., Ossipov, M.H., Aurora, S.K., 2019. CGRP and the trigeminal system in migraine. Headache. 59, 659–681. https://doi.org/10.1111/head.13529.

Kelman, L., 2004. The place of osmophobia and taste abnormalities in migraine classification: a tertiary care study of 1237 patients. Cephalalgia. 24, 940–946. https://doi.org/10.1111/j.1468-2982.2004.00766.x.

Koroleva, V.I., Bures, J., 1980. Blockade of cortical spreading depression in electrically and chemically stimulated areas of cerebral cortex in rats. Electroencephalogr. Clin. Neurophysiol. 48, 1–15. https://doi.org/10.1016/0013-4694(80)90038-3.

Leao, A.A.P., 1944. Spreading depression of activity in the cerebral cortex. J. Neurophysiol. 7, 359–390. https://doi.org/10.1152/jn.1944.7.6.359.

Li, J., Vause, C.V., Durham, P.L., 2008. Calcitonin gene-related peptide stimulation of nitric oxide synthesis and release from trigeminal ganglion glial cells. Brain Res. 1196, 22–32. https://doi.org/10.1016/j.brainres.2007.12.028.

Lu, C.X., Qiu, T., Liu, Z.F., Su, L., Cheng, B., 2017. Calcitonin gene-related peptide has protective effect on brain injury induced by heat stroke in rats. Exp. Ther. Med. 14, 4935–4941. https://doi.org/10.3892/etm.2017.5126.

McKinney, W., Van Der Walt, S., Millman, J., 2010. Data structures for statistical computing in python. In: Proceedings of the 9th Python in Science Conference, pp. 51–56 doi:10.25080/MAJORA-92BF1922-00A.

Messlinger, K., 2018. The big CGRP flood - sources, sinks and signalling sites in the trigeminovascular system. J. Headache Pain. 19, 22. https://doi.org/10.1186/s10194-018-0848-0.

Na, H., Gan, Q., Mcparland, L., Yang, J.B., Yao, H., Tian, H., Zhang, Z., Qiu, W.Q., 2020. Characterization of the effects of calcitonin gene-related peptide receptor antagonist for Alzheimer's disease. Neuropharmacology. 168, 108017. https://doi.org/10.1016/j.neuropharm.2020.108017.

Nicholson, C., 1993. Ion-selective microelectrodes and diffusion measurements as tools to explore the brain cell microenvironment. J. Neurosci. Methods 48, 199–213. https://doi.org/10.1016/0165-0270(93)90092-6.

Olsson, T., Broberg, M., Pope, K.J., Wallace, A., Mackenzie, L., Blomstrand, F., Nilsson, M., Willoughby, J.O., 2006. Cell swelling, seizures and spreading depression: an impedance study. Neuroscience. 140, 505–515. https://doi.org/10.1016/j.neuroscience.2006.02.034.

Patel, D.C., Tewari, B.P., Chaunsali, L., Sontheimer, H., 2019. Neuron-glia interactions in the pathophysiology of epilepsy. Nat. Rev. Neurosci. 20, 282–297. https://doi.org/10.1038/s41583-019-0126-4.

Petrusic, I., Zidverc-Trajkovic, J., Podgorac, A., Sternic, N., 2013. Underestimated phenomena: higher cortical dysfunctions during migraine aura. Cephalalgia. 33, 861–867. https://doi.org/10.1177/0333102413476373.

Reback, J., McKinney, W., Brockmendel, J., Van den Bossche, J., Augspurger, T., Cloud, P., Young, G.F., Sinhrks, Klein, A., Roeschke, M., Hawkins, S., Tratner, J., She, C., Ayd, W., Petersen, T., Garcia, M., Schendel, J., Hayden, A., MomIsBestFriend, Jancauskas, V., Battiston, P., Seabold, S., Chris, B., Vetinari, H., Hoyer, S., Overmeire, W., Alimcmaster, Dong, K., Whelan, C., Mehyar, M., 2020. pandas-dev/pandas: Pandas 1.0.3 (v1.0.3). Zenodo, 10.5281/zenodo.3715232.

Rehni, A.K., Singh, T.G., Jaggi, A.S., Singh, N., 2008. Pharmacological preconditioning of the brain: a possible interplay between opioid and calcitonin gene related peptide transduction systems. Pharmacol. Rep. 60, 904–913. https://if-pan.krakow.pl/pjp/pdf/2008/6_904.pdf.

Richter, F., Lütz, W., Eitner, A., Leuchtweis, J., Lehmenkühler, A., Schaible, H.G., 2014. Tumor necrosis factor reduces the amplitude of rat cortical spreading depression in vivo. Ann. Neurol. 76, 43–53. https://doi.org/10.1002/ana.24176.

Richter, F., Eitner, A., Leuchtweis, J., Bauer, R., Lehmenkühler, A., Schaible, H.G., 2017. Effects of interleukin-1β on cortical spreading depolarization and cerebral vasculature. J. Cereb. Blood Flow Metab. 37, 1791–1802. https://doi.org/10.1177/0271678X16641127.

Richter, F., Eitner, A., Leuchtweis, J., Bauer, R., Ebersberger, A., Lehmenkühler, A., Schaible, H.G., 2018. The potential of substance P to initiate and perpetuate cortical spreading depression (CSD) in rat in vivo. Sci. Rep. 8, 17656. https://doi.org/10.1038/s41598-018-36330-2.

Risch, M., Vogler, B., Dux, M., Messlinger, K., 2021. CGRP outflow into jugular blood and cerebrospinal fluid and permeance for CGRP of rat dura mater. J. Headache Pain. 22, 105. https://doi.org/10.1186/s10194-021-01320-9.

Russell, F.A., King, R., Smillie, S.J., Kodji, X., Brain, S.D., 2014. Calcitonin gene-related peptide: physiology and pathophysiology. Physiol. Rev. 94, 1099–1142. https://doi.org/10.1152/physrev.00034.2013.

Ryu, P.D., Gerber, G., Murase, K., Randic, M., 1988. Actions of calcitonin gene-related peptide on rat spinal dorsal horn neurons. Brain Res. 441, 357–361. https://doi.org/10.1016/0006-8993(88)91414-x.

Saklani, P., Khan, H., Gupta, S., Kaur, A., Singh, T.G., 2022. Neuropeptides: potential neuroprotective agents in ischemic injury. Life Sci. 288, 120186. https://doi.org/10.1016/j.lfs.2021.120186.

Schneider, C.A., Rasband, W.S., Eliceiri, K.W., 2012. NIH image to ImageJ: 25 years of image analysis. Nat. Methods 9, 671–675. https://doi.org/10.1038/nmeth.2089.

Shibata, M., Suzuki, N., 2017. Exploring the role of microglia in cortical spreading depression in neurological disease. J. Cereb. Blood Flow Metab. 37, 1182–1191. https://doi.org/10.1177/0271678X17690537.

Shimazaki, K., Yajima, T., Ichikawa, H., Sato, T., 2022. Distribution and possible function of galanin about headache and immune system in the rat dura mater. Sci. Rep. 12, 5206. https://doi.org/10.1038/s41598-022-09325-3.

Silberstein, S.D., 1995. Migraine symptoms: results of a survey of self-reported migraineurs. Headache. 35, 387–396. https://doi.org/10.1111/j.1526-4610.1995.hed3507387.x.

Silberstein, S.D., 2004. Migraine. Lancet. 363, 381–391. https://doi.org/10.1016/S0140-6736(04)15440-8.

Syková, E., 2004. Extrasynaptic volume transmission and diffusion parameters of the extracellular space. Neuroscience. 129, 861–876. https://doi.org/10.1016/j.neuroscience.2004.06.077.

Taylor, F.R., 2019. CGRP, amylin, immunology, and headache medicine. Headache. 59, 131–150. https://doi.org/10.1111/head.13432.

Teppola, H., Acimovic, J., Linne, M.L., 2019. Unique features of network bursts emerge from the complex interplay of excitatory and inhibitory receptors in rat neocortical networks. Front. Cell. Neurosci. 13, 377. https://doi.org/10.3389/fncel.2019.00377.

Thalakoti, S., Pati, L.V.V., Damodaram, S., Vause, C.V., Langford, L.E., Freeman, S.E., Durham, P.L., 2007. Neuron-glia signaling in trigeminal ganglion: implications for migraine pathology. Headache. 47, 1008–1123. https://doi.org/10.1111/j.1526-4610.2007.00854.x.

Ting, J.T., Daigle, T.L., Chen, Q., Feng, G., 2014. Acute brain slice methods for adult and aging animals: application of targeted patch clamp analysis and optogenetics. Methods Mol. Biol. 1183, 221–242. https://doi.org/10.1007/978-1-4939-1096-0_14.

Van Rossum, G., Drake Jr., F.L., 1995. Python Reference Manual. Centrum voor Wiskunde en Informatica, Amsterdam.

Vinogradova, L.V., 2018. Initiation of spreading depression by synaptic and network hyperactivity: insights into trigger mechanisms of migraine aura. Cephalalgia. 38, 1177–1187. https://doi.org/10.1177/0333102417724151.

Wang, Y., Tye, A.E., Zhao, J., Ma, D., Raddant, A.C., Bu, F., Spector, B.L., Winslow, N.K., Wang, M., Russo, A.F., 2019. Induction of calcitonin gene-related peptide expression in rats by cortical spreading depression. Cephalalgia. 39, 333–341. https://doi.org/10.1177/0333102416678388.

Warfvinge, K., Edvinsson, L., 2019. Distribution of CGRP and CGRP receptor components in the rat brain. Cephalalgia. 39, 342–353. https://doi.org/10.1177/0333102417728873.

Waskom, M.L., 2021. seaborn: statistical data visualization. J. Open Source Software. 60, 3021. Doi: 10.21105/joss.03021.

Wimalawansa, S.J., 1996. Calcitonin gene-related peptide and its receptors: molecular genetics, physiology, pathophysiology, and therapeutic potentials. Endocr. Rev. 17, 533–585. https://doi.org/10.1210/edrv-17-5-533.

Young, K., Morrison, H., 2018. Quantifying microglia morphology from photomicrographs of immunohistochemistry prepared tissue using ImageJ. J. Vis. Exp. 5, 57648. https://doi.org/10.3791/57648.

Zheng, F., Nixdorf-Bergweiler, B.E., van Brederode, J., Alzheimer, C., Messlinger, K., 2021. Excitatory effects of calcitonin gene-related peptide (CGRP) on superficial Sp5C neurons in mouse medullary slices. Int. J. Mol. Sci. 22, 3794. https://doi.org/10.3390/ijms22073794.